Metallaboranes with Group 8 and 9 Transition Metals. ## Is Accurate *ab initio* Molecular Orbital Calculation of Structure, Stability, and NMR Chemical Shifts Possible?

Alexander M. MEBEL,#,† Djamaladdin G. MUSAEV,†,†† Nobuaki KOGA,†,††† and Keiji MOROKUMA*,†,††

† Institute for Molecular Science, Myodaiji, Okazaki 444

†† Cherry L. Emerson Center for Scientific Computation and Department of Chemistry, Emory University, Atlanta, GA 30322, U.S.A.

††† College of General Education and Graduate School of Human Informatics, Nagoya University, Nagoya 464-01

(Received May 13, 1993)

Ab initio MO study of structure, stability and rearrangements of nido-metallaboranes with Ir, Co, and Fe transition metals has been performed at HF and correlated MP2 levels. Reasonable agreement with experiment has been found for RHF optimized geometry of $[(IrB_5H_8)(CO)(PH_3)_2]$ iridaborane, and the MP2 optimization improves the agreement to the maximum error of 0.035 Å. Two geometric isomers, 2- with basal Ir and 1- with apical Ir are close in energy for $[(IrB_5H_8)(CO)(PH_3)_2]$. NMR ^{11}B and ^1H chemical shifts calculated by the IGLO method qualitatively reproduce experimental spectra. Methods more sophisticated than MP2 would be necessary for accurate calculations of metallaboranes with first row transition metals.

Novel metallaboranes and metallacarboranes are being described with increasing frequency.[1—7] Borane and carborane ligands are shown to be of value as ligands in organometallic synthesis allowing creation of new kinds of stable metallaboranes and, potentially, new materials having novel electronic, magnetic or optical properties.[1,8] Also, analogy between boranes and metal clusters allows information on the former to be used to provide a first order picture of the behavior of the latter. Metallaboranes, lying in the middle, have been assigned a key role in relating structure of borane clusters to those of metal clusters and to metal–hydrocarbon π-complexes.[9]

Recent *ab initio* calculations on polyhedral boranes,[10—14] carboranes[15,16] and heteroboranes with hetero atoms of sp-elements[17—21] as well as on boron clusters by late Hiroshi Kato[22] appear to be very useful in elucidation of their stability, geometric and electronic structure, NMR ^{11}B chemical shifts and other properties. Theoretical studies of metallaboranes with transition metals have been limited only to extended Hückel and Fenske–Hall investigations.[23] These methods do not describe reliably geometric structure and stability of the clusters. Thus, metallaboranes remain to be challenging objects for *ab initio* MO study.

Preparation, structure and NMR spectral data of 2-$[(IrB_5H_8)(CO)(PPh_3)_2]$ were reported[24] in 1979. In the metal–boron cluster the iridium and five boron atoms form a pentagonal pyramid in which the iridium atom is in a basal position. The atomic disposition resembles that of B_6H_{10}, distorted to accommodate the larger iridium atom and with omission of a bridging hydrogen. Some other geometric isomers are possible for this compound but have not been observed.

Possibility of existence of some isomers differing in disposition of distinct atoms in a skeleton is a typical property of structure of clusters for all metallaboranes. Isomerization is well-known for carboranes[25,26] and some examples have been reported for metallaboranes. The cobaltaborane isomers, 1- and 2-$[(\eta^5\text{-}C_5H_5)Co]B_4H_8$, are structural and electronic analogs of pentaborane(9), B_5H_9, in which a $Co(C_5H_5)$ unit replaces a BH group at an apical and a basal position, respectively. These compounds were first isolated[27] as the red crystalline, air stable 2-isomer and found to thermally rearrange to 1-isomer, a pale yellow crystal. Geometric structures of both isomers were determined later by X-ray crystallographic method.[28,29]

2-$[(\eta^5\text{-}C_5H_5)Fe]B_5H_{10}$ ferraborane was obtained in 1977 and from ^{11}B and ^1H NMR spectra it was assigned to a pentagonal-pyramidal structure with iron atom in the base and five bridging hydrogen atoms (3 B–H–B's and 2 Fe–H–B's) on the open face.[30] Upon heating, this compound rearranged to 1-$[(\eta^5\text{-}C_5H_5)Fe]$-$B_5H_{10}$, in which the iron atom is proposed to occupy the apex position.[31] Both isomers are electronic analogs of hexaborane(10), B_6H_{10}, and 1-isomer is a direct structural analog of ferrocene and contains a cyclic $B_5H_{10}^-$ ligand, isoelectronic with $C_5H_5^-$. $Fe(B_5H_{10})_2$ has been isolated only as 2,2′-isomer, suggested on the basis of NMR ^{11}B and ^1H observation.[32] Other possible geometric isomers, e.g. 1,1′ and 1,2′, have not been reported. X-ray structural analysis of the ferraboranes has not been performed.

We now present the first *ab initio* MO study of metallaboranes. Our objectives were to find adequate approximations for calculations of metallaboranes, to determine geometric structure and relative stabilities of different isomers of the compounds, and to study their electronic structure and the binding character between transition metals and borane ligands.

##This paper is dedicated to late Professor Hiroshi Kato.

#On leave from Institute of New Chemical Problems, Russian Academy of Science, Chernogolovka, Moscow Region, Russia, 142432.

Methods

The geometries of different structures of metallaboranes were fully optimized in a given symmetry at the restricted Hartree–Fock (HF) and in many cases at the correlated Møller–Plesset second order perturbation (MP2) level.[33] For Ir atom we use the Hay–Wadt effective core potential, called ECP17, which takes explicitly into account 17 electrons in $nsnpnd(n+1)s(n+1)p$ shells,[34] together with the valence [3s3p2d]/(5s5p3d) basis set. For Fe and Co we use the basis set suggested by Wachters[35] supplemented with diffuse p-functions and d-functions from the basis set of Rappe,[36] resulting in the contraction [8s8p3d]/(14s11p6d). The effective core potential (ECP5) was used for P atoms with the [2s2p]/(3s3p) valence basis set.[37] For the other non-metallic atoms (B, C, H, etc.) the standard 6-31G[33] basis set was employed. Below we denote this overall basis set as I. In some cases we also performed calculations with the basis set, denoted as II, which is set I supplemented by polarization d-functions on boron atoms. In some case we have also carried out single point calculations as MP3/I and MP4(SDQ)/I levels. All the calculations were performed with GAUSSIAN90[38] and GAUSSIAN92[39] programs.

Results and Discussion

I. Iridaborane. $(IrB_5H_8)(CO)(PH_3)_2$. Geometries and Relative Energies of Isomers. The iridaborane cluster, $[(IrB_5H_8)(CO)(PPh_3)_2]$, may be regarded as formally derived from B_6H_{10} by the replacement of a bridging hydrogen and a BH group by Ir-$(CO)(PPh_3)_2$ fragment. From this point of view, six different geometric configurations, shown in Fig. 1, are possible for the iridaborane. The notation of each structure represents the number of the boron atom replaced from the parent B_6H_{10} hexaborane. The isomer (**2**) is found experimentally.[24] The structures (**3a**) and (**3b**) differ from each other by removal of left or right bridge hydrogen with respect to the position (3). In (**4**) coordination number of the metal atom is six, whereas it is seven in (**2**) and (**3**). In the configurations (**1**) and (**1a**) Ir is situated in the apical position and has formal coordination number eight. One of the bridging hydrogens in the base of a pentagonal pyramid is removed; in (**1a**) all three remaining bridges are adjacent, and in (**1**) two are adjacent and one is isolated. In our study we simulate the experimentally observed iridaborane by $[(IrB_5H_8)(CO)(PH_3)_2]$.

It has been shown for a large series of nido- and arachno-boranes that the MP2/6-31G* method usually reproduces experimental geometric parameters with reliability of 0.01—0.02 Å.[13] We have recently demonstrated that this method provides a similar accuracy in calculation of geometries of Lewis base adducts of smallest nido-boranes, B_3H_7 and B_4H_8.[40] Less time-consuming MP2/6-31G approximation gives worse results and usually overestimates BB distances in borane frameworks by up to 0.05—0.06 Å. In principle, we could expect a similar reliability at the same levels of theory

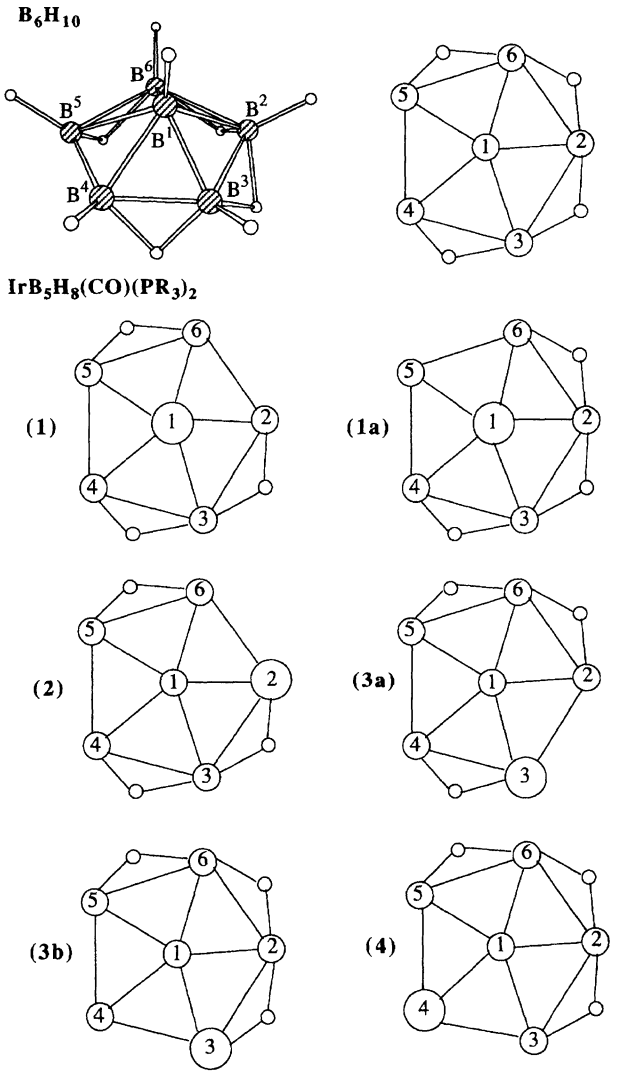

Fig. 1. Possible geometric configurations of $[(IrB_5H_8)(CO)(PR_3)_2]$, where a large circle represents the Ir-$(CO)(PR_3)_2$ group, medium circles BH groups, and small circles bridging hydrogen atoms.

also for metallaboranes. In order to find an adequate method, at the beginning we have performed calculations of the iridaborane **2** isomer for which experimental geometry is available. Three different approximations have been employed for geometry optimization, HF/I, MP2/I, and MP2/II. The optimized structures are shown in Fig. 2, and geometric parameters are collected in Table 1. Even at the simplest HF/I level we have found reasonable agreement with experiment for geometry of IrB_5 metallaborane framework. The largest deviation is 0.059 Å for B^1B^4 distance, and the average deviation is 0.031 Å. MP2/I slightly improves the results to the maximum error of 0.045 Å and the average error of 0.028 Å, and MP2/II makes them closer to the X-ray data with errors of 0.035 Å and 0.026 Å, respectively. Since the results of HF/I optimization have qualitatively acceptable reliability for **2**, for the other configurations we carried out optimization only at this

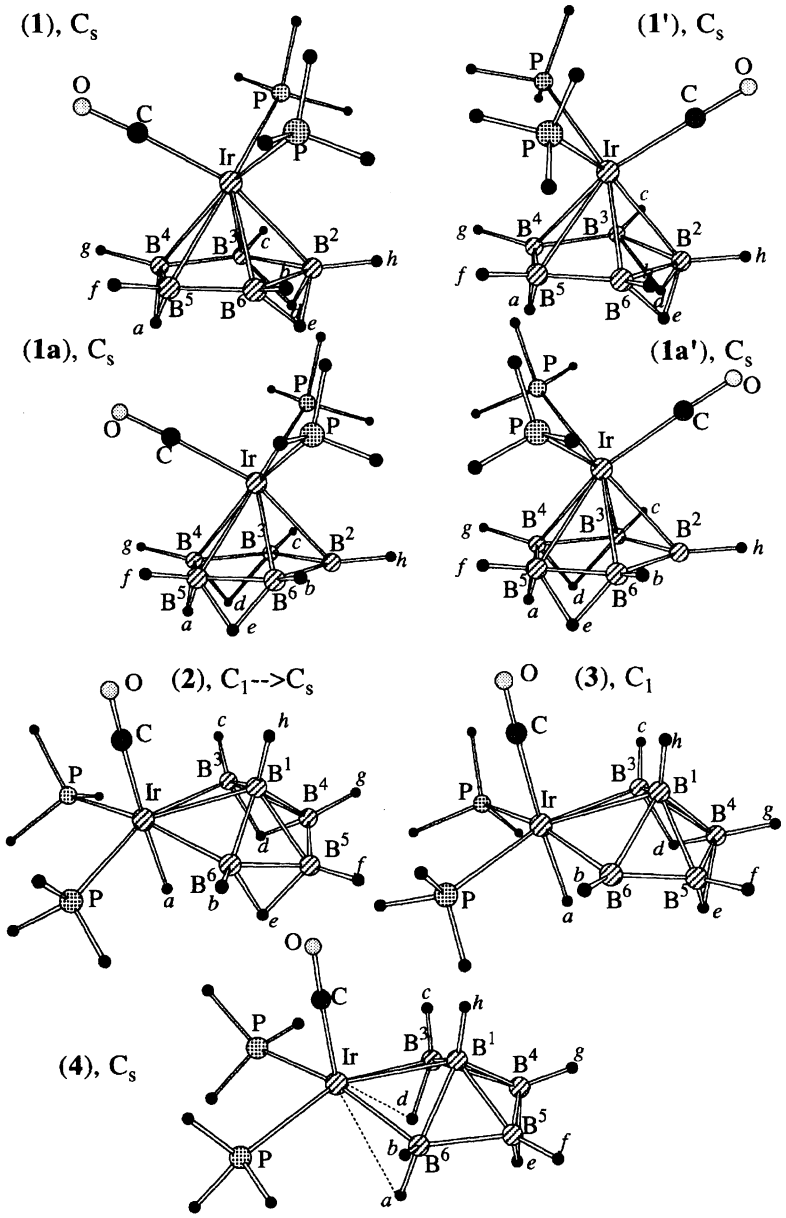

Fig. 2. Different optimized structures of $[(IrB_5H_8)(CO)(PH_3)_2]$.

level of theory. RHF wavefunctions for optimized structures were subjected to stability test calculations, and all of them were found to be stable to becoming UHF wavefunctions, an indication of closed shell nature of the state.

The main difference of concern between the calculated and the experimental crystalline structure of 2-$[(IrB_5H_8)(CO)(PR_3)_2]$, **2** is position of the bridging hydrogen between Ir and B^3. At all three levels of theory, optimizing under C_1 symmetry, the initial structure converged to a structure very close to C_s symmetry, with the H atom bound only with iridium. MP2/II calculation reproduces, meanwhile, the experimental value of Ir–H bond length. Although the solid state X-ray structure requires that five boron atoms and eight hydrogen atoms in the cluster be all chemically distinct and therefore they should exhibit separate ^{11}B and ^1H NMR signals, experimental NMR spectra in solution show no difference between B^3 and B^6, between B^4 and B^5, between H^b and H^c, between H^f and H^g, and between two bridge hydrogens, H^d and H^e.[24] It has been suggested[24] that either accidental equivalence of chemical shifts occurs, or the structure is in dynamic equilibrium in solution, i.e. the Ir–H^a–B bridging hydride alternates between Ir–B^3 and Ir–B^6 positions thus rendering the pairs of boron and hydrogen atoms chemically equivalent on a time-average. However, no further multiplicity in the NMR spectrum has been found even at −70 °C. Our calculations suggest that there is no dynamic equilibrium of the hydrogen between B^3 and B^6 atoms, but rather that the equilibrium geometry of the isolated molecule is in C_s symmetry. There must be a difference in the iridaborane geometry between solution or gas phase and solid state.

Table 1. Energies and Geometries of Different Configurations of $[(IrB_5H_8)(CO)(PH_3)_2]$ (Bond Lengths are in Å, Angles are in Degrees)

	(**2**) $C_1 \rightarrow C_s$				(**3**) C_1	(**4**) C_s	(**1**) C_s	(**1′**) C_s	(**1a**) C_s	(**1a′**) C_s	B_6H_{10}[e] C_s	
	HF/I	MP2/I[b]	MP2/II[c]	exp.[d]	HF/I	HF/I	HF/I	HF/I	HF/I	HF/I	MP2/6-31G*	
E_{tot}	−360.	−361.	−360.		−360.	−360.	−360.	−360.	−360.	−360.	−154.	
	45932	43785	61720		43603	39929	44785	45060	43359	43437	43224	
E_{tot},[a] a.u.												
(MP2/I	−361.				−361.	−361.	−361.	−361.	−361.	−361.		
//HF/I)	41622				39423	35180	41841	42235	40439	40068		
E_{rel}, kcal mol^{-1}												
HF	0.0				14.5	37.7	7.2	5.5	16.1	15.7		
MP2	0.0				13.8	40.4	−2.4	−3.8	7.4	9.8		
$IrB^{1(2)}$	2.311	2.301	2.243	2.278	2.383	2.317	2.199	2.203	2.454	2.541	B^1B^2	1.741
IrB^3	2.217	2.235	2.218	2.250	2.205	2.232	2.294	2.251	2.375	2.293		
$IrB^{6(4)}$	2.205	2.231	2.214	2.183	2.184	2.232	2.330	2.348	2.171	2.199		
IrH^a	1.621	1.667	1.734	1.73	1.630	2.388	2.918	3.008	2.822	2.895		
IrC	1.961	1.894	1.823	1.873	1.953	1.847	1.947	1.928	1.941	1.946		
IrP	2.485	2.407	2.398	2.400	2.466	2.532	2.448	2.454	2.442	2.451		
	2.425	2.391	2.402	2.349	2.444	2.532	2.448	2.454	2.442	2.451		
CO	1.139	1.197	1.204	1.150	1.139	1.142	1.141	1.141	1.141	1.141		
$B^{1(2)}B^3$	1.744	1.773	1.770	1.747	1.700	1.856	1.933	1.907	1.639	1.661	B^1B^3	1.748
$B^{1(2)}B^4$	1.840	1.826	1.785	1.781	1.731	1.721	2.889	2.855	2.948	2.983	B^1B^4	1.800
$B^{1(2)}B^5$	1.837	1.826	1.787	1.793	1.801	1.721	2.889	2.855	2.948	2.983	B^2B^3	1.782
$B^{1(2)}B^6$	1.756	1.775	1.765	1.772	1.977	1.856	1.933	1.907	1.639	1.661		
B^3B^4	1.740	1.732	1.678	1.711	1.765	1.820	1.620	1.661	1.907	1.955	B^3B^4	1.732
B^4B^5	1.684	1.697	1.679	1.649	1.791	1.652	1.985	1.840	1.977	1.827	B^4B^5	1.638
B^5B^6	1.740	1.734	1.682	1.708	1.654	1.820	1.620	1.661	1.907	1.955		
B^2H^d							1.310	1.302			B^2H^{23}	1.298
B^2H^e							1.310	1.302				
B^3H^a	2.446	2.431	2.422	1.41	2.520						B^3H^{23}	1.369
B^3H^d	1.372	1.371	1.354	1.39	1.342	1.236	1.336	1.339	1.358	1.387	B^3H^{34}	1.327
B^4H^a							1.318	1.319	1.329	1.320	B^4H^{34}	1.329
B^4H^d	1.309	1.320	1.307	1.28	1.345				1.288	1.277		
B^4H^e					1.418	1.344						
B^5B^a							1.318	1.319	1.329	1.320		
B^5H^e	1.321	1.322	1.305	1.31	1.296	1.344			1.288	1.277		
B^6H^a	2.470	2.437	2.428		2.351	1.236						
B^6H^e	1.366	1.368	1.353	1.29			1.336	1.339	1.358	1.387		
P^1IrP^2	98.0	98.1	94.4	106.0	97.4	100.5	93.3	93.1	93.6	96.0		
P^1IrC	97.1	97.4	101.4	92.1	97.6	94.5	96.9	96.8	96.7	95.1		
P^2IrC	96.9	97.7	101.5	97.3	96.0	94.5	96.9	96.8	96.7	95.1		
$CIrB^{1(2)}$	82.6	84.6	90.3	90.0	83.0	83.6	162.3	83.9	167.4	77.5		
$CIrB^3$	100.7	102.0	107.0	128.4	94.9	105.4	118.7	108.1	133.7	93.9		
$CIrB^{6(4)}$	99.3	101.7	106.2	82.7	102.3	105.4	84.8	150.1	89.9	144.8		
$CIrH^a$	177.5	176.6	178.3	167.	176.0	135.6						
IrCO	179.1	179.1	179.5	174.9	178.0	178.1	177.6	178.1	177.7	179.9		

a) Total energy of single point calculations at MP2/I level with valence electrons only correlated (frozen core) and with HF/I optimized geometry. b) Geometry optimization at MP2(full)/I level with all electrons correlated. c) Geometry optimization at MP2(full)/II level. Basis set II contains 5d basis functions, while set I uses 6d. d) Experimental X-ray geometry taken from Ref. 24. e) Data from Ref. 13. Superscript numbers for H atoms correspond to the numbers of boron atoms in Fig. 1 with which the hydrogens are bound.

Optimizations starting from (**3a**) and (**3b**) both give the same isomer **3** in C_1 symmetry as shown in Fig. 2 and Table 1. The H^a atom again does not like the bridging position between iridium and boron atoms but prefers to bind only to Ir. It is situated a little closer to B^6 than to B^3, with the corresponding non-bonding distances of 2.35 and 2.52 Å, respectively. Geometry of **3** is quite similar to that of **2**, but differs only by the position of one bridging hydrogen. The optimized structure of **4** in C_s differs from those of **2** and **3**; H^a and H^d atoms have left the initial bridging positions and are involved into BH_2 groups at B^3 and B^6. Interestingly, agostic interactions are found between iridium and these two hydrogens; $Ir–H^{a,d}$ distances are 2.39 Å, and the $B^3–H^d$ and $B^6–H^a$ bonds are elongated by about 0.05 Å as compared with the regular terminal B–H bond length. However, the agostic hydrogens are not quite at bridging positions between Ir and B.

For each of (**1**) and (**1a**) with axial disposition of iridium atom in the metallaborane, we found two optimized structures in C_s symmetry. In **1** and **1a** CO and B^2 ligands on the metal atom are in trans position, and in **1′** and **1a′** they are located in cis position. Geometries of these apical-Ir structures significantly deviate from that of the reference B_6H_{10} borane. In addition to longer distances compared to the borane apical-equatorial B^1–B bond distances expected by Ir atomic size, the basal part of the borane framework is strongly distorted under Ir influence. Bridged B–B bond lengths (1.83—1.99 Å) in these structures are up to 0.20 Å longer than those in B_6H_{10}, while non-bridged B–B bond lengths (1.62—1.66 Å) remain unchanged. Noteworthy, B–B distances cis to CO undergo the largest elongation.

At the HF/I level the experimentally found **2** is the most stable, and **1** and **1′** lie 5—7 kcal mol^{-1} higher in energy. Electron correlation stabilizes the apical-Ir structures, and at the MP2/I//HF/I level, i.e. MP2/I with HF/I optimized geometries, **1′** becomes the most stable structure. At higher levels of perturbation theory **1′** is stabilized further, and lies 7.5 and 8.6 kcal mol^{-1} lower than **2** in MP3/I and MP4(SDQ)/I approximations. It means that **1′** is thermodynamically the most stable isomer and experimentally found **2** isomer is not. Experimental finding of **2**, but not **1′** may be due to the way of synthesis. The iridaborane was prepared in the reaction,

$$K[B_5H_8] + [Ir(CO)Cl(PPh_3)_2] \rightarrow KCl + [(IrB_5H_8)(CO)(PPh_3)_2],$$

and, according to Greenwood[24] it could proceed via an initially formed iridium μ-2,3-nido-pentaborane intermediate in which Ir occupies a bridging position in the base of tetragonal pyramidal frame of $B_5H_8^-$, and then cluster expansion into pentagonal pyramid takes place. Only **2** isomer could be formed this way. Some other synthetic approaches could result in formation of **1′**.

Energy difference between **1** and **1′** is very small, 1—2 kcal mol^{-1}, so is that between **1a** and **1a′**. Hence, rotation of the distorted borane moiety on the Ir atom is nearly free in the Ir-apical isomers, within **1** and **1′** and also within **1a** and **1a′**. The structure **3** is about 14 kcal mol^{-1} less stable than **2**, and structures **1** and **1′** are 10—13 kcal mol^{-1} more favorable than **1a** and **1a′**. It means that bridging hydrogens do not like to occupy adjacent positions; the smaller number of neighboring bridges, the more stable configuration of the iridaborane. Configuration **4** lies very high in energy and probably is not a local minimum.

Stereochemistry of Iridium Atom. As shown in Fig. 3, in all calculated configurations Ir atom displays distorted octahedral stereochemistry. One also notes that PH_3 ligands are cis to each other and cis to CO. In structures **2** and **3**, where Ir is basal, the position trans to CO is occupied by H^{Ir} hydride. The two remaining coordination sides trans to phosphines are occupied by a tridentate B_5H_7 ligand with B^1B^3 bond at one position and B^1B^6 at the second.

In the configurations **1** and **1a**, B^2 is trans to CO, while B^3B^4 and B^5B^6 bonds are trans to phosphines. In **1′** and **1a′**, with rotation of $Ir(CO)(PH_3)_2$ moiety, B^4B^5 bond becomes trans to CO, and B^2B^3 and B^2B^6 are trans to phosphines.

Electronic Structure of the Iridaborane. Greenwood et al.[24] suggested two alternative approaches to the description of the electronic structure within the iridaborane cluster. The first one is to consider $[(IrB_5H_8)(CO)(PPh_3)_2]$ as derivative of B_6H_{10} where one neutral BH group and a neutral bridging hydrogen, which together supply three skeletal electrons, are substituted by a neutral d^9 $Ir(CO)(PPh_3)_2$ moiety. According to electron counting rules for boranes,[9] a

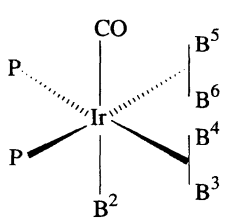

1, 1a

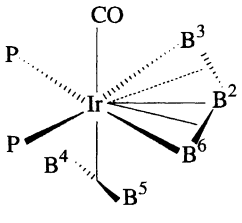

1′, 1a′

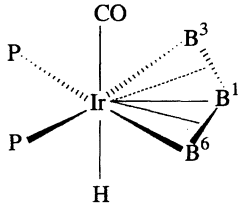

2, 3

Fig. 3. Stereochemistry of Ir atom in the iridaborane.

Table 2. Mulliken Population Analysis[a] of Different Configurations of $[(IrB_5H_8)(CO)(PH_3)_2]$

	(**2**), C_1	(**3**), C_1	(**4**), C_s	(**1**), C_s	(**1′**), C_s	(**1a**), C_s	(**1a′**), C_s	$IrCO(PH_3)_2$	B_6H_{10}[b]
Ir	−1.69	−1.70	−0.74	−1.67	−1.57	−1.56	−1.52	−0.28	
Q_s, Ir	1.13	1.12	0.95	1.01	0.98	0.97	0.99	0.85	
Q_p, Ir	7.54	7.56	7.19	7.73	7.67	7.69	7.61	6.70	
Q_d, Ir	10.02	10.02	9.60	9.93	9.92	9.90	9.92	9.73	
$B^{1(2)}$	−0.04	−0.03	+0.09	+0.18	+0.19	+0.37	+0.29		−0.17
B^3	+0.49	+0.40	+0.17	+0.23	+0.26	+0.08	+0.19		−0.04
B^4	+0.02	+0.01	+0.02	+0.22	+0.18	+0.23	+0.17		+0.03
B^5	+0.02	−0.10							B^2:−0.06
B^6	+0.50	+0.61							H^1:+0.03
H^{Ir}	+0.27	+0.26	−0.03						H^3:+0.04
C	+0.47	+0.47	+0.43	+0.51	+0.47	+0.49	+0.48	+0.35	H^4:+0.00
O	−0.45	−0.45	−0.45	−0.45	−0.45	−0.45	−0.45	−0.48	H^2:+0.04
P	+0.35	+0.34	+0.28	+0.37	+0.36	+0.37	+0.35	+0.24	H^{23}:+0.04
$IrCO(PH_3)_2$	−0.97	−0.97	−0.09	−0.85	−0.77	−0.71	−0.75	0.00	H^{34}:+0.00
B_5H_8	+0.97	+0.97	+0.09	+0.85	+0.77	+0.71	+0.75		
Q, $IrB^{1(2)}$	0.13	0.15	0.15	0.01	0.06	−0.01	−0.00		
Q, IrB^3	−0.17	−0.03	0.14	0.07	−0.01	0.03	−0.04		
Q, $IrB^{6(4)}$	−0.20	−0.04		−0.00	0.03	0.00	0.09		
Q, IrH^{Ir}	0.29	0.32	−0.00						
Q, IrC	0.03	0.03	0.13	0.18	0.14	0.21	0.17	0.16	
Q, IrP	0.11	0.12	0.16	0.16	0.19	0.18	0.14	0.13	

a) Numbers without label are net atomic charges and their sums over atoms. Q are orbital population and bond population.
b) Superscript numbers for H atoms correspond to the numbers of boron atoms in Fig. 1 with which the hydrogens are bound.

transition metal fragment contributes $\nu+x-12$ skeletal electrons, where ν is the number of valence electrons of a metal, and x is the number of electrons donated by ligands. As a result, this iridium moiety supplies also three electrons to the polyhedral skeleton and the compound may be regarded as a d^6 iridium(III) species, consistent with octahedral stereochemistry just discussed above.

An alternative formal approach is to regard the species as a derivative of arachno-pentaborane(11), B_5H_{11}. Removal of three protons from B_5H_{11} yields the arachno-anion $[B_5H_8]^{3-}$ which interacts with the d^6 cation $[Ir(CO)(PPh_3)_2]^{3+}$. This cation contributes an additional vertex but no additional bonding electrons to the cluster and therefore converts the arachno-pentaborane species into a nido-hexaborane derivative.

Calculated Mulliken populations are summarized in Table 2. In all calculated isomers Ir atom has high negative charge, from −1.52 to −1.70 e. The $Ir(CO)(PH_3)_2$ fragment has a charge close to −1 e, while B_5H_8 ligand is correspondingly positively charged. Thus, the first approach seems to be more realistic. In going from B_6H_{10} to various configurations of $[(IrB_5H_8)(CO)(PH_3)_2]$, one BH group together with one bridging H atom is replaced by $Ir(CO)(PH_3)_2$. If one calculates from Table 2 the Mulliken charge of a BH_2 unit to be replaced, one finds +0.02, +0.04 or −0.00 and +0.03 for B^2H_2, B^3H_2, and B^4H_2, respectively, which can be compared with −0.14 or −0.10 for B^1H_2. Calculated energetical preference of **1′** isomer of the iridaborane over **2** may in part reflect the fact that B^1 position is a little richer in negative charge than the other positions. At any position, the Ir moiety actually substitutes a neutral BH and H and therefore requires one electron donated from the rest of B_5H_8 ligand.

Table 2 shows that population on d-orbitals of Ir atom in the iridaborane is close to 10 and is only slightly larger than that in neutral $Ir(CO)(PH_3)_2$ fragment. One notices, however, that population of p-orbitals has increased almost by 1e in $[(IrB_5H_8)(CO)(PH_3)_2]$, and the main growth of negative charge on iridium occurs through p-orbitals. Electron density comes from H^{Ir} atom and adjacent borons (B^3, B^6) in Ir-basal configurations **2** and **3**, and from all basal B atoms in **1** and its family when Ir is located in the apical position. Charges on B atoms next to iridium become as large as +0.5e. Thus, in spite of its electron deficiency, borane ligand serves as an electron donor providing electrons mainly to vacant p-orbitals of the Ir atom.

^{11}B NMR Chemical Shift. Recently, an *ab initio* perturbation method using the IGLO program[41] has been applied with some considerable success in the determination of ^{11}B and ^{13}C chemical shifts at MO-optimized structures of boron hydrides,[13] closoboranes,[14,17,42,43] carboranes,[13—16,44] and Lewis base adducts of small boranes;[40] the predicted shifts agree very well with experimental results. We have examined whether this procedure can be used to compute

^{11}B, ^{1}H, and ^{13}C chemical shifts for metallaboranes. In our calculations we used Huzinaga DZ[45] basis sets for sp-elements as well as the previous mentioned Hay–Wadt pseudopotentials and basis sets[34] for transition metals.

Calculated chemical shifts for 2-$[(IrB_5H_8)(CO)(PH_3)_2]$ are compared with experimental results for 2-$[(IrB_5H_8)(CO)(PPh_3)_2]$[24] in Table 3. Such a comparison is reasonable because, as have been shown for $B_4H_8PR_3$,[40] nature of phosphine ligands has little effect on chemical shifts in the cluster skeleton. Since acceptable agreement has been found between optimized and X-ray structures of the iridaborane, with the exception of the position of H^{Ir}, IGLO calculations for isomer **2** have been carried out for three different geometries: experimental, HF/I, and MP2/II. Qualitative agreement with experimental NMR ^{11}B shifts is found for all the cases. The best agreement is obtained for chemical shifts calculated at the MP2/II geometry. They are significantly closer to the experimental values than those calculated with experimental X-ray geometry. This supports our conclusion made in a previous section that the structure of 2-$[(IrB_5H_8)(CO)(PR_3)_2]$ in solution or gas phase differs from the crystalline geometry by the position of hydrogen between Ir and B^3. However, reliability of the calculated ^{11}B chemical shifts is not as high as found for usual boranes and carboranes.[13—16,40] The largest discrepancy of DZ//MP2/II calculated values from experiment reaches 10 ppm for B^1, and the average deviation is 6.6 ppm. Probably, larger basis sets are necessary for more accurate calculations, or correlation effects on geometry are more significant in chemical shift calculation for metallaboranes than for boron hydrides.

Table 3. Calculated NMR ^{11}B, and ^{1}H Chemical Shifts for 2-$[(IrB_5H_8)(CO)(PH_3)_2]$ (ppm, Relative to $BF_3{\cdot}OEt_2$ for ^{11}B, and TMS for ^{1}H)

	DZ//RHF/I	DZ//RMP2/II	DZ//exp.[a]	exp. δ[b]
B^1	−17.1	−17.7	−40.1	−28±3
B^3	+44.5		+28.7	
B^6	+43.2		+33.5	
(B^3,B^6) [c]	+43.9	+39.1	+31.1	+42±3
B^4	+20.1		+11.8	
B^5	+21.4		+21.7	
(B^4,B^5) [c]	+20.8	+16.7	+16.8	+10±3
H^h	+1.2	+1.5	−3.1	−0.4
H^c	+7.7		+7.0	
H^b	+7.5		+5.9	
(H^b,H^c) [c]	+7.6	+7.4	+6.6	+6.7
H^g	+5.3		+5.0	
H^f	+5.4		+5.4	
(H^f,H^g) [c]	+5.4	+5.3	+5.2	+4.9
H^a	−12.6	−7.7	−11.8	−12.1
H^d	−4.7		−4.5	
H^e	−4.8		−7.2	
(H^d,H^e) [c]	−4.7	−5.2	−5.9	−2.6

a) At experimental X-ray geometry for 2-$[(IrB_5H_8)(CO)(PPh_3)_2]$ from Ref. 24. b) Experimental chemical shifts for 2-$[(IrB_5H_8)(CO)(PPh_3)_2]$ from Ref. 24. c) Averaged value.

The agreement of theoretical and experimental chemical shifts for hydrogen atoms is also satisfactory. The order of chemical shifts for different kinds of protons is calculated correctly. Proton chemical shifts for terminal hydrogens are reproduced with reliability of 1—2 ppm. The chemical shift for the critical H^{Ir} atom is better for HF/I and X-ray geometry, but at MP2/II geometry it deviates from the experimental value as much as 4 ppm. This result can not be used for conclusion about the location of this atom; in the HF/I optimized structure the hydrogen is bound only with Ir, in the X-ray structure it occupies the bridging position, and yet the chemical shift values are very close.

Concluding Remarks. Our calculations of the iridaborane demonstrate that, for metallaboranes with third row transition metal, geometry optimization at the HF level with effective core potential including outermost core orbitals for a transition metal atom and a basis set of DZ quality can give qualitatively acceptable results. Taking into account electron correlation at MP2 level and including polarization d-functions on B atoms into the basis set make discrepancies between the theoretical geometric parameters and experimental data rather small.

Two geometric isomers, one with Ir in basal position and another in apical position, are found for $[(IrB_5H_8)(CO)(PH_3)_2]$. While **2** isomer has been observed experimentally, **1′** is predicted to be thermodynamically more stable and further synthetic attempts are encouraged. Ir atom in the iridaborane has octahedral stereochemistry and a large negative charge, with borane B_5H_8 serving as electron donor.

II. Metallaboranes with First Row Transition Metals. [(η^5-Cyclopentadienyl)-cobalta-nido-pentaborane], $Co(C_5H_5)B_4H_8$. The cobaltaborane isomers, 1- and 2-$[(\eta^5\text{-}C_5H_5)Co]B_4H_8$ with a $Co(C_5H_5)$ unit in an axial or an equatorial position, are shown in Fig. 4. Comparison of optimized geometric parameters, collected in Table 4, with experimental X-ray data[28,29] demonstrates obvious inadequacy of the RHF method in correctly reproducing CoC, CoB, and CoH^b bond lengths. For instance, in (**2**)-isomer the CoC, CoB^2, and CoH^b distances are overestimated by 0.2—0.3 Å. For (**1**)-isomer correspondence of calculated RHF geometry with experiment is better, but CoC bond lengths are again overestimated by 0.13 Å. The picture is similar to that found by Almlöf for first row transition metal metallocenes;[46] in cobaltacene, for example, RHF optimized Co–Cp ring separation was 0.23 Å longer than the experimental one.

RMP2 optimization significantly improves the results, though discrepancies remain noticeable for Co–Cp fragment as well as for CoB_4 framework. Both

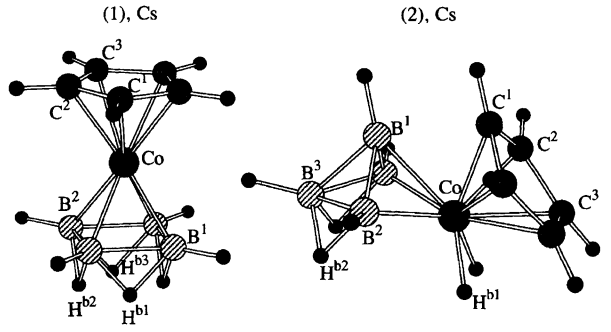

Fig. 4. Optimized geometric structures of $Co(C_5H_5)$-B_4H_8.

Table 4. Geometries and Energies of Different Structures of $Co(C_5H_5)B_4H_8$ (Bond Lengths in Å)

	(1), C_s			(2), C_s		
	RHF/I[a]	MP2/I[b]	exp.[c]	RHF/I[a]	MP2/I[b]	exp.[d]
E_{tot}, a.u.	−1676. 56295	−1677. 75949		−1676. 60363	−1677. 75305	
E_{rel}, kcal mol^{-1}	25.5	0.0		0.0	4.0	
CoB^1	2.023	1.905	1.977	2.017	2.051	2.007
CoB^2	2.021	1.900	1.977	2.317	2.046	2.135
CoH^{b1}				1.723	1.520	1.429
B^1B^1	1.824	1.894	1.834			
B^1B^2	1.820	1.895	1.834	1.748	1.744	1.685
B^1B^3				1.749	1.737	1.660
$B^2B^{2(3)}$	1.825	1.899	1.834	1.793	1.769	1.757
$B^{1(2)}H^{b1}$	1.345	1.369	1.315	1.274	2.553	1.434
B^1H^{b2}	1.345	1.369	1.259			
B^2H^{b2}	1.346	1.372	1.259	1.359	1.333	1.300
B^2H^{b3}	1.345	1.371	1.315			
B^3H^{b2}				1.322	1.373	1.092
CoC^1	2.190	1.941	2.069	2.215	1.934	2.018
CoC^2	2.192	1.956	2.069	2.210	2.001	2.006
CoC^3	2.193	1.982	2.069	2.258	2.001	2.062
C^1C^2	1.417	1.472	1.401	1.419	1.479	1.389
C^2C^3	1.416	1.470	1.401	1.421	1.483	1.397
C^3C^3	1.417	1.461	1.401	1.411	1.542	1.387

a) The basis set I is [8s8p3d]/(14s11p6d) for Co and 6-31G for B, C, and H. b) RMP2(frozen core)/I geometry optimization. c) Experimental X-ray data from Ref. 29. d) Experimental X-ray data from Ref. 28.

Co–B and Co–C distances are usually underestimated by 0.07—0.13 Å, with only exception of CoB^1 bond length in (**2**)-isomer calculated 0.04 Å longer than in experiment. Almlöf's MP2 calculations of ferrocene with larger basis set including f-functions give Fe–Cp distance 0.08 Å shorter than the experimental value and dynamic correlation via modified coupled-pair functional (MCPF) was found to be necessary to reproduce experiment properly.[47] This appears to be the case for the cobaltaborane for which similar deviations have been observed. Inclusion of polarization d-functions would decrease B–B and C–C bond lengths by 0.05—0.06 Å. Thus, quantitatively correct description of geometry of group 8 and 9 first row transition metal metalloboranes would require a large basis set and a correlation approach more sophisticated than MP2.

Both (**1**)- and (**2**)-isomers of $Co(C_5H_5)B_4H_8$ at RMP2/I geometry have RHF wavefunctions unstable to becoming UHF. Such instability has been found also for $FeCp_2$,[48] for which a quintet state lies about 57 kcal mol^{-1} lower than a singlet after annihilation of triplet at the projected unrestricted MP3 (PUMP3) level, in spite that ferrocene is experimentally known to be diamagnetic. Such a failure has been ascribed to the poorly calculated energy difference between the ground state ($^5D(s^2d^6)$ for Fe) and the excited state (^1D (d^8) for Fe) responsible for strong binding.

RHF instability of 1-$Co(C_5H_5)B_4H_8$ is negligible; UHF singlet lies only 0.04 kcal mol^{-1} lower than RHF singlet, and triplet and quintet states are 29.5 and 84.2 kcal mol^{-1} higher, while negative eigenvalue of stability matrix and $<S^2>$ after annihilation are close to zero. For isomer (**2**), however, the instability is very substantial; while triplet and quintet are 43.4 and 58.5 kcal mol^{-1} less stable than RHF singlet, UHF singlet is lower in energy than RHF singlet by 20.9 kcal mol^{-1}, and $<S^2>$ is as large as 5.04 after annihilation of triplet. RHF approximation gives (**2**)-isomer of $Co(C_5H_5)B_4H_8$ more stable than (**1**) by 25.5 kcal mol^{-1}, but the electron correlation reversed the order; (**2**) becomes 4.0 kcal mol^{-1} higher than (**1**) at RMP2/I. Electron correlation, probably, improves the energy separation of metal atomic states, as discussed above. However, PUMPn calculations would be useful for singlet state of (**2**)-structure to de-contaminate high spin contributions for more reliable description of the energy. On the base of our results, one can say that calculated energy difference between (**1**)- and (**2**)-isomers is not very large in accord with experimental evidence of (**2**)→(**1**) transformation upon heating up to 175—200 °C.

In the X-ray experiment[29] C_5H_5 ring in (**1**)-isomer is disordered, and the molecule crystal has an imposed four-fold axis; the B_4 ring is therefore constrained to square planar geometry, parallel to $C_5H_5^-$ ligand. But local symmetry of the CoB_4H_8 fragment is lower than C_{4v} due to asymmetry of the B–H–B bridges. On the other hand, NMR ^{11}B and ^1H spectra showed that all bridge hydrogens as well as terminal H's and boron atoms are respectively equivalent. RMP2 optimization of geometry of 1-$Co(C_5H_5)B_4H_8$ in C_s symmetry converges to C_{4v} local symmetry of CoB_4H_8 with almost equivalent bridging hydrogens and C_{5v} local symmetry of CoC_5H_5 fragment, and makes B_4 square and C_5 pentagon planar, in agreement with NMR observation but contradicting to apparent difference of bridge hydrogens in the X-ray experiment. The asymmetry of the bridges might be due to bias of crystal forces or an artifact caused by experimental difficulties in determination of H atoms. The terminal hydrogens on the B_4H_8

ligand are slightly out of the B_4 plane, by 3° both in experiment and our calculations, in contrast to parent B_5H_9 where these atoms are substantially bent toward the apex (24° by experiment). Our calculation of (**1**)-isomer with C_5H_5 turned around the five-fold axis by 45° toward an eclipsed structure, with other geometric parameters frozen, leads to increase of the total energy only by 0.04 kcal mol^{-1}.

Interesting difference between calculated and X-ray structure of 2-Co(C_5H_5)B_4H_8[28] is position of bridging hydrogens between metal and boron atoms. At RMP2 optimized geometry of (**2**) these H's are bound only with Co and do not interact with B^2. This also suggests possible deviations of crystalline structure from those in gas phase or solution.

Mulliken population analysis for CoCp and CoCp-B_4H_8, given in Table 5, shows that B_4H_8 ligand is an electron donor, and there are σ- and π-donations from B_4H_8 to metal, and δ-back donation in the opposite direction. CoCp and B_4H_8 have proper frontier orbitals for such type of interactions; for the former those are mostly vacant p-orbitals and occupied d-orbitals of the metal atom, as shown in Fig. 5. While σ-donation is comparable, π-donation is stronger for (**2**), but δ-back donation is stronger for (**1**) isomer. In general, Co atom acquires negative charge, and B_4H_8 ligand attains positive charge in the metalloborane. Part of electron density on Co comes also from cyclopentadienyl. The largest increase in electron density is found on p-orbitals of the metal atom.

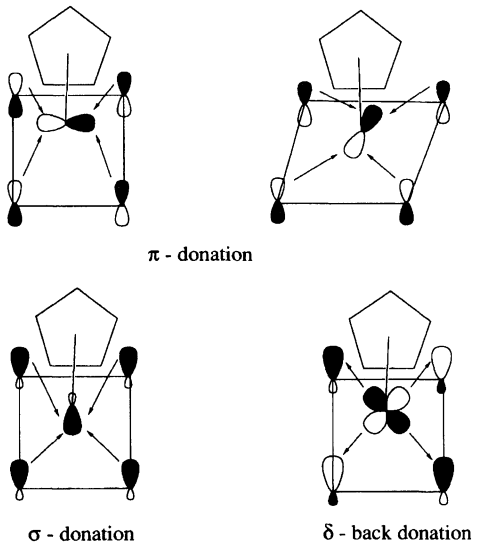

Fig. 5. Structure of frontier orbitals in CoC_5H_5 and B_4H_8 fragments of the cobaltaborane.

Table 5. Mulliken Population Analysis[a] for CoC_5H_5 and Co(C_5H_5)B_4H_8

	CoC_5H_5	$CoC_5H_5B_4H_8$	
		(**1**)	(**2**)
Co	+0.39	−0.78	−1.55
Q_{4s}, Co	0.20	0.67	0.78
Q_{4p}, Co	0.39	1.15	1.60
Q_{4d}, Co	8.02	7.96	8.17
Q_σ, Co	2.29	3.15	3.20
Q_π, Co	2.37	3.58	4.02
Q_δ, Co	3.95	3.05	3.33
B^1		+0.03	−0.02
B^2		+0.03	+0.19
B^3			−0.01
C^1	−0.27	−0.16	−0.16
C^2		−0.15	−0.09
C^3		−0.14	−0.08
H^{b1}		+0.03	+0.19
H^{b2}		+0.03	0.00
H^{b3}		+0.03	
C_5H_5	−0.39	+0.41	+0.79
B_4H_8		+0.37	+0.76
Q, CoB^1		0.07	0.08
Q, CoB^2		0.05	0.12
Q, CoH^{b1}			0.31
Q, CoC^1	0.06	−0.01	0.07
Q, CoC^2		−0.01	−0.03
Q, CoC^3		−0.00	0.01

a) Numbers without label are net atomic charges and their sums over atoms. Q are orbital population and bond population.

Since agreement of the RMP2 optimized geometry with experiment is not very good for Co(C_5H_5)B_4H_8, we used for IGLO calculations X-ray determined atomic coordinates which are available for (**1**)-isomer. Calculated chemical shifts are shown in Table 6. The discrepancy of the theoretical ^{11}B chemical shift from experiment is about 5 ppm. For ^{13}C it is significantly larger, and the reason of this deviation must be deficiency of the RHF wavefunction, used for IGLO calculations, in description of bonding in the first row transition metal–Cp interaction. Excellent agreement with experiment has been found for ^{1}H chemical shifts of terminal hydrogens with B and C atoms. However, the negative shift for the bridging hydrogens is not reproduced well, a situation similar to iridaborane in Table 3.

Ferraboranes, Fe(C_5H_5)B_5H_{10} and Fe(B_5H_{10})$_2$. Our calculations of the ferraboranes are only prelimi-

Table 6. Calculated NMR ^{11}B, ^{1}H, and ^{13}C Chemical Shifts for 1-[Co(C_5H_5)B_4H_8] (ppm, Relative to BF_3·OEt_2 for ^{11}B, and TMS for ^{1}H and ^{13}C)

	DZ//exp.[a]	exp. δ[b]
B	−9.8	−4.4
H^t	+1.8	+2.8
H^b	−13.4	−4.3
H(Cp)	+5.0	+5.0
C	+65.8	+83.2

a) At experimental X-ray geometry from Ref. 29.
b) Experimental chemical shifts from Ref. 29.

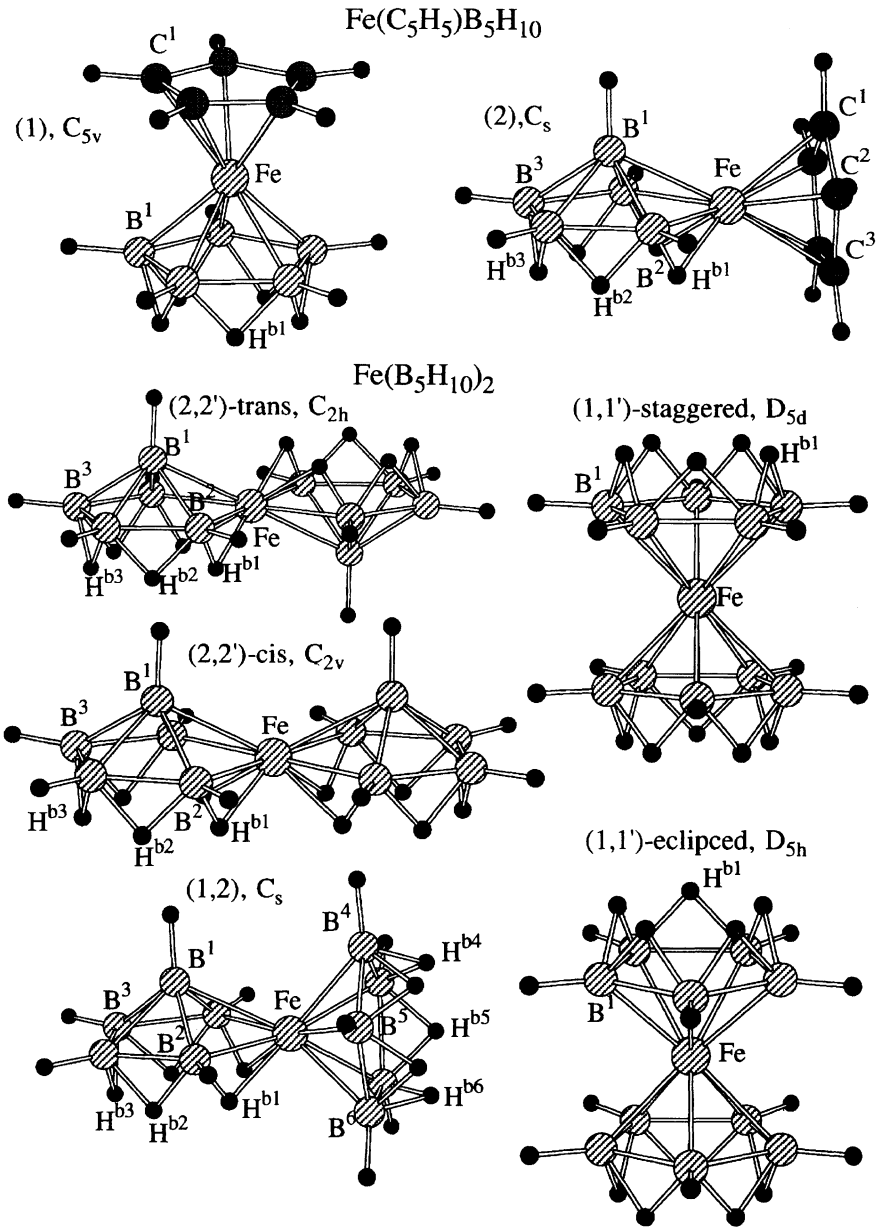

Fig. 6. Optimized geometric structures of $Fe(C_5H_5)B_5H_{10}$ and $Fe(B_5H_{10})_2$.

nary. For $Fe(C_5H_5)B_5H_{10}$ we considered two isomers shown in Fig. 6, in a basal and an axial position. Both of them are known experimentally.[31] For $Fe(B_5H_{10})_2$ five possible distinct configurations shown in Fig. 6 have been calculated, cis- and trans-(2,2′)-structures, eclipsed and staggered (1,1′)-structures, and (1,2′)-structures. The RHF optimized parameters are shown in Table 7.

As in the case of ferrocene, geometric structures of the ferraboranes are difficult to calculate. Experimental X-ray data are not available for $Fe(C_5H_5)B_5H_{10}$ but RHF results are obviously not sufficiently reliable. For instance, calculated Fe–C distances are 2.26—2.30 Å, but experimental value for ferrocene is 2.06 Å.[49] In $[(Et_2C_2B_4H_4)FeH-(C_5Me_4)]_2C_6H_4$ ferracarborane X-ray measured[50] bond lengths between Fe and C in Cp* rings are also 2.06—2.07 Å, and therefore this distance should not be noticeably different in ferraboranes and ferracarboranes. As in ferrocene case, RHF approximation overestimates Fe–Cp separation by 0.20—0.25 Å. The Fe–B bond length is usually in the range of 2.15—2.25 Å in ferraboranes and ferracarboranes,[50] where our RHF results fall. However, FeB^1 bond length of 2.41 Å in (**2**) is obviously overestimated. RHF wavefunctions for both isomers of $Fe(C_5H_5)B_5H_{10}$ are significantly unstable, and quintets appear to be the ground states lying 40—45 kcal mol^{-1} lower than RHF singlets. It means that at least PUMP2 calculations of singlet and quintet states are necessary for correct description of geometry and relative energies of the isomers of $Fe(C_5H_5)B_5H_{10}$.

This is the case also for $Fe(B_5H_{10})_2$. But we can suggest some cautionary conclusions about the struc-

Table 7. Geometries and Energies of Different Configurations of $Fe(C_5H_5)B_5H_{10}$ and $Fe(B_5H_{10})_2$ Optimized at the RHF/I Level. Bond Lengths are in Å

	$Fe(C_5H_5)B_5H_{10}$		$Fe(B_5H_{10})_2$					
	(**1**), C_{5v}	(**2**), C_s	(1,1′)		(1,2′)		(2,2′)	
			stagg., D_{5d}	eclip., D_{5h}			trans, C_{2h}	cis, C_{2v}
E_{tot}, a.u.	−1583. 43520	−1583. 52437	−1520. 27608	−1520. 27315	−1520. 36070		−1520. 45124	−1520. 40129
E_{rel}, kcal mol^{-1}	55.9	0.0	109.9	111.8	56.8		0.0	31.3
FeB^1	2.169	2.409	2.184	2.191	2.439		2.424	2.416
FeB^2		2.289			2.305		2.309	2.321
FeH^{b1}		1.842			1.848		1.855	1.873
$FeC^1(B^4)$	2.262	2.304			2.165			
$FeC^2(B^5)$		2.282			2.281			
$FeC^3(B^6)$		2.290			2.235			
B^1B^2	1.792	1.801	1.787	1.788	1.803		1.809	1.808
B^1B^3		1.768			1.764		1.768	1.770
B^2B^3		1.808			1.821		1.803	1.806
B^3B^3		1.772			1.761		1.774	1.762
$B^2H^{b1}[B^4H^{b4}]$	1.334	1.238	1.333	1.332	1.233	[1.440]	1.239	1.241
$B^2H^{b2}[B^5H^{b4}]$		1.391			1.406	[1.272]	1.390	1.374
$B^3H^{b2}[B^5H^{b5}]$		1.288			1.299	[1.314]	1.292	1.298
$B^3H^{b3}[B^6H^{b6}]$		1.339			1.336	[1.346]	1.340	1.337
$C^1C^2(B^4B^5)$	1.415	1.412			1.747			
$C^2C^3(B^5B^6)$		1.428			1.914			
$C^3C^3(B^6B^6)$		1.405			1.715			

ture of this species. Experimental geometry of (2,2′) was proposed only on the base of NMR observation,[32] but the pattern of spectra should be the same for cis-(C_{2v}) and trans-(C_{2h}) configurations. At RHF level trans-structure lies 31 kcal mol^{-1} lower than cis-, and relative energy should not be very dependent on the approximation because steric factors here would be most important. Thus, trans-(2,2′) conformation is probably a local minimum, and cis-(2,2′) corresponds to a rotational barrier about the horizontal axis. The second conclusion is possibility of free mutual rotation of FeB_5H_{10} moieties around the five-fold axis in (1,1′)-configuration, suggested by nearly equal energies of eclipsed (D_{5h}) and staggered (D_{5d}) structures.

In general, accurate calculations of ferraborane clusters seem to be very difficult and time consuming and should be performed with extreme care, with taking into account of low lying higher spin states. In many cases more sophisticated than MP2 correlation methods will be necessary for correct description of wavefunctions of ferraboranes.

The present research is supported in part by Grants-in-Aid from Ministry of Education, Science and Culture. DGM acknowledges Postdoctoral Fellowship from the Japan Society for the Promotion of Science. Some numerical calculations were carried out at the Computer Center, Institute for Molecular Science.

References

1) R. N. Grimes, *Chem. Rev.*, **92**, 251 (1992).
2) G. Fergusson, J. F. Gallagher, M. McGrath, J. P. Sheelan, T. R. Spalding, and J. D. Kennedy, *J. Chem. Soc., Dalton Trans.*, **1993**, 27.
3) A. R. Oki, H. Zhang, J. A. Maguire, N. S. Hosmane, H. Ro, W. E. Hatfield, M. Moscherosch, and W. Kaim, *Organometallics*, **11**, 4202 (1992).
4) N. W. Alcock, I. D. Burns, K. S. Claire, and A. F. Hill, *Inorg. Chem.*, **31**, 4606 (1992).
5) J. Bould, J. D. Kennedy, and W. S. McDonald, *Inorg. Chim. Acta*, **196**, 201 (1992).
6) K. E. Stockman, M. Sabat, M. G. Finn, and R. N. Grimes, *J. Am. Chem. Soc.*, **114**, 8733 (1992).
7) F. A. Gomez, S. E. Johnson, C. B. Knobler, and M. F. Hawthorne, *Inorg. Chem.*, **31**, 3558 (1992).
8) J. Plesek, *Chem. Rev.*, **92**, 269 (1992).
9) C. E. Housecroft and T. P. Fehlner, *Adv. Organomet. Chem.*, **21**, 57 (1982).
10) M. L. McKee, *J. Phys. Chem.*, **93**, 3426 (1989).
11) M. L. McKee, *J. Phys. Chem.*, **94**, 435 (1990).
12) J. Cioslowski and M. L. McKee, *J. Phys. Chem.*, **96**, 9264 (1992).
13) M. Bühl and P. v.R. Schleyer, *J. Am. Chem. Soc.*, **114**, 477 (1992).
14) M. Bühl, A. M. Mebel, O. P. Charkin, and P. v.R. Schleyer, *Inorg. Chem.*, **31**, 3769 (1992).
15) J. W. Bausch, G. K. Surya Prakash, and R. E. Williams, *Inorg. Chem.*, **31**, 3763 (1992).
16) T. Onak, J. Tseng, D. Tran, S. Herrera, B. Chan, J.

Arias, and M. Diaz, *Inorg. Chem.*, **31**, 3910 (1992).
17) M. Bühl, P. v.R. Schleyer, Z. Havlas, D. Hnyk, and S. Hermanek, *Inorg. Chem.*, **30**, 3107 (1991).
18) R. Zahradnik, V. Balaji, and J. Michl, *J. Comput. Chem.*, **12**, 1147 (1991).
19) M. L. McKee, *J. Phys. Chem.*, **95**, 9273 (1991).
20) E. D. Jemmis, G. Subramanian, and L. Radom, *J. Am. Chem. Soc.*, **114**, 1481 (1992).
21) M. L. McKee, *J. Phys. Chem.*, **96**, 1679 (1992).
22) H. Kato, K. Yamashita, and K. Morokuma, *Chem. Phys. Lett.*, **190**, 361 (1992).
23) See for example: P. Brint and T. R. Spalding, *J. Chem. Soc., Dalton Trans.*, **1980**, 1236; T. P. Fehlner, P. T. Czech, and R. F. Fenske, *Inorg. Chem.*, **29**, 3103 (1990).
24) N. N. Greenwood, J. D. Kennedy, W. S. McDonald, D. Reed, and J. Staves, *J. Chem. Soc., Dalton Trans.*, **1979**, 117.
25) R. E. Williams, in "Progress in Boron Chemistry," ed by R. J. Brotherton, H. Steinberg, Pergamon, Oxford (1970), Vol. 2, p. 37.
26) B. M. Gimarc and J. J. Ott, *Main Group Metal Chem.*, **12**, 77 (1989).
27) V. R. Miller, R. Weiss, and R. N. Grimes, *J. Am. Chem. Soc.*, **99**, 5646 (1977).
28) L. G. Sneddon and D. Voet, *J. Chem. Soc., Chem. Commun.*, **1975**, 118.
29) T. L. Venable, E. Sinn, and R. N. Grimes, *J. Chem. Soc., Dalton Trans.*, **1984**, 2275.
30) R. Weiss and R. N. Grimes, *J. Am. Chem. Soc.*, **99**, 8087 (1977).
31) R. Weiss and R. N. Grimes, *Inorg. Chem.*, **18**, 3291 (1979).
32) S. G. Shore, J. Ragaini, T. Schmitkons, L. Barton, G. Medford, and J. Plotkin, "Abstr. IMEBORON, 4th," (1979), p. 36.
33) W. J. Hehre, L. Radom, P. v.R. Schleyer, and J. A. Pople, "*Ab initio* Molecular Orbital Theory," Wiley, New York (1986).
34) P. J. Hay and W. R. Wadt, *J. Chem. Phys.*, **82**, 299 (1985).
35) A. J. H. Wachters, *J. Chem. Phys.*, **52**, 1033 (1970).
36) A. K. Rappe, T. A. Smedley, and W. A. Goddard, III, *J. Phys. Chem.*, **85**, 2607 (1981).
37) W. R. Wadt and P. J. Hay, *J. Chem. Phys.*, **82**, 284 (1985).
38) M. J. Frisch, M. Head-Gordon, G. W. Trucks, J. B. Foresman, H. B. Schlegel, K. Raghavachari, M. Robb, J. S. Binkley, C. Gonzales, D. J. DeFrees, D. J. Fox, R. A. Whiteside, R. Seeger, C. F. Melius, J. Baker, R. L. Martin, L. R. Kahn, J. J. P. Stewart, S. Topiol, and J. A. Pople, "Gaussian 90," Gaussian, Inc., Pittsburgh, PA (1990).
39) M. J. Frisch, G. W. Trucks, M. Head-Gordon, P. M. W. Gill, M. W. Wong, J. B. Foresman, B. G. Johnson, H. B. Schlegel, M. A. Robb, E. S. Replogle, R. Gomperts, J. L. Andres, K. Raghavachari, J. S. Binkley, C. Gonzales, R. L. Martin, D. J. Fox, D. J. DeFrees, J. Baker, J. J. P. Stewart, and J. A. Pople, "Gaussian 92," Gaussian, Inc., Pittsburgh, PA (1992).
40) A. M. Mebel, D. G. Musaev, and K. Morokuma, *Chem. Phys. Lett.*, submitted for publication.
41) W. Kutzelnigg, *Isr. J. Chem.*, **19**, 193 (1980); M. Schindler and W. Kutzelnigg, *J. Chem. Phys.*, **76**, 1919 (1982); W. Kutzelnigg, U. Fleischer, and M. Schindler, in "NMR, Basic Principles and Progress," Springer Verlag, Berlin (1990), p. 165.
42) A. M. Mebel, O. P. Charkin, M. Bühl, and P. v.R. Schleyer, *Inorg. Chem.*, **32**, 463 (1993).
43) A. M. Mebel, O. P. Charkin, and P. v.R. Schleyer, *Inorg. Chem.*, **32**, 469 (1993).
44) T. Onak, J. Tseng, M. Diaz, D. Tran, J. Arias, S. Herrera, and D. Brown, *Inorg. Chem.*, **32**, 487 (1993).
45) S. Huzinaga, "Approximate Atomic Wave Functions," University of Alberta, Edmonton, Alberta, Canada (1971).
46) J. Almlöf, K. Faegri, B. Schilling, and H. P. Lüthi, *Chem. Phys. Lett.*, **106**, 266 (1984).
47) G. Park and J. Almlöf, *J. Chem. Phys.*, **95**, 1829 (1991).
48) M. L. McKee, *J. Phys. Chem.*, **96**, 1683 (1992).
49) A. Haaland and J. E. Nilsson, *Acta Chem. Scand.*, **22**, 2653 (1968).
50) M. Stephan, J. H. Davis, Jr., X. Meng, and R. N. Grimes, *J. Am. Chem. Soc.*, **114**, 5399 (1992).